AUTHOR QUERY FORM

AIP Publishing	**Journal: J. Chem. Phys.** **Article Number: JCP19-AR-CQD2019-03179**	**Please provide your responses and any corrections by annotating this PDF and uploading it to AIP's eProof website as detailed in the Welcome email.**

Dear Author,

Below are the queries associated with your article. Please answer all of these queries before sending the proof back to AIP.

Article checklist: In order to ensure greater accuracy, please check the following and make all necessary corrections before returning your proof.
1. Is the title of your article accurate and spelled correctly?
2. Please check affiliations including spelling, completeness, and correct linking to authors.
3. Did you remember to include acknowledgment of funding, if required, and is it accurate?

Location in article	Query/Remark: click on the Q link to navigate to the appropriate spot in the proof. There, insert your comments as a PDF annotation.
Q1	Please check that the author names are in the proper order and spelled correctly. Also, please ensure that each author's given and surnames have been correctly identified (given names are highlighted in red and surnames appear in blue).
Q2	We have reworded the sentence beginning "However, a monolayer of. . ." for clarity. Please check that your meaning is preserved.
	Please confirm ORCIDs are accurate. If you wish to add an ORCID for any author that does not have one, you may do so now. For more information on ORCID, see https://orcid.org/. Mona Rafipoor – Hans Tornatzky – 0000-0002-3153-0501 Dorian Dupont – Janina Maultzsch – Mickael D. Tessier – Zeger Hens – Holger Lange – 0000-0002-4236-2806
	Please check and confirm the Funder(s) and Grant Reference Number(s) provided with your submission: Deutsche Forschungsgemeinschaft, Award/Contract Number EXC 2056—Project No. 390715994, EXC 1074—Project No. 194651731 Please add any additional funding sources not stated above.

Thank you for your assistance.

Strain in InP/ZnSe, S core/shell quantum dots from lattice mismatch and shell thickness—Material stiffness influence

View Online   Export Citation   CrossMark

Mona Rafipoor,[1] Hans Tornatzky,[2] (ID) Dorian Dupont,[3] Janina Maultzsch,[2] Mickael D. Tessier,[3] Zeger Hens,[3] and Holger Lange[1,a) (ID)

AFFILIATIONS

[1]Institut für Physikalische Chemie, Universität Hamburg, Hamburg, Germany
[2]Institut für Physik der Kondensierten Materie, Friedrich-Alexander Universität Erlangen Nürnberg, Erlangen, Germany
[3]Physics and Chemistry of Nanostructures, Department of Chemistry, Ghent University, Ghent, Belgium

Note: This paper is part of the JCP Special Topic on Colloidal Quantum Dots.
[a)]Electronic mail: Holger.Lange@chemie.uni-hamburg.de

ABSTRACT

We investigate the buildup of strain in InP quantum dots with the addition of shells of the lower-lattice constant materials ZnSe and ZnS by Raman spectroscopy. Both materials induce compressive strain in the core, which increases with increasing shell volume. We observe a difference in the shell behavior between the two materials: the thickness-dependence points toward an influence of the material stiffness. ZnS has a larger Young's modulus and requires less material to develop stress on the InP lattice at the interface, while ZnSe requires several layers to form a stress-inducing lattice at the interface. This hints at the material stiffness being an additional parameter of relevance for designing strained core/shell quantum dots.

Published under license by AIP Publishing. https://doi.org/10.1063/1.5124674

I. INTRODUCTION

Most photonic applications of colloidal semiconductor quantum dots (QDs) employ core/shell nanocrystals.[1–4] The shell passivates the sensitive core, allows circumventing QD blinking, and generally improves the QD's optical properties.[5] Among the potential II–VI and III–V compound semiconductor materials for QDs, InP offers a broad emission wavelength range, robust synthesis protocols, and high stability.[5,6] Core/shell InP/ZnSe and InP/ZnS QDs display favorable photoluminescence properties in combination with a lower toxicity than for Cd-based QDs.[7–9]

In most cases, core/shell QDs are strained materials because of surface reconstruction compensating the lattice mismatch between the core and the shell.[10] The strain can lead to the formation of defects that give rise to localized electronic states in the bandgap, increasing the rate of nonradiative recombinations and, by that, the quantum yield. However, strain can also be used as an additional parameter to tune light emission by QDs.[11–13] The control and optimization of the core/shell strain is therefore of general interest. Changing the lattice constants allows us to engineer the strain, for example, by using quaternary solid solutions such as Zn, Cd and S, Se.[14,15]

In addition to the mismatch between the two lattices, the core size and the shell dimensions are relevant parameters for the induced strain.[16,17] In general, smaller cores and shells are more strained, where larger structures have more possibilities to relax strain within the material. This leads to complex dependencies, complicating the minimization of strain or the use of strain for material engineering.

Raman spectroscopy is a powerful tool to investigate strain in QDs. It is a nondestructive, room-temperature experiment that requires only a small sample amount. Regarding strain, Raman spectroscopy does not suffer from the limited element sensitivity of transmission electron microscopy (TEM) and has a higher sensitivity than powder X-ray diffraction. In most cases, it can address

the core and shell simultaneously and also delivers information on alloying and further structural properties.[15–20]

In the present study, we focus on InP core/shell QDs and investigate the interplay between strain and the shell thickness and lattice mismatch for the two most established shell materials, ZnS and ZnSe. For both shells, the lattice mismatch leads to compressive strain in the core. However, a monolayer of ZnS already shows a strong impact, whereas ZnSe shells only induce a more drastic strain buildup with increasing shell thickness. This difference in the thickness dependence can be understood when considering the material stiffness as a relevant parameter in addition to the previously mentioned lattice mismatch and sizes.

II. METHODS

A. Synthesis

The synthesis protocol for InP/ZnSe QDs was reported earlier.[21] For bare InP QDs and the InP/ZnS QDs, we employed a protocol modified by us.[15] We used InP QDs with 3.2 nm diameter as cores. The core diameter was estimated using a combination of bright field transmission electron microscopy (TEM) and absorption spectroscopy, as described in the supplementary material. Aliquots were taken during different steps of the shell growth for obtaining different shell thicknesses. ZnSe shells with 2, 5, 9, and 13 monolayers were synthesized. In addition, InP/ZnS QDs with 1, 2, and 3 shell monolayers were prepared. TEM images were taken using a JEOL 2200 FS microscope, and absorption spectra were taken using a Perkin Elmer Lambda 950 spectrometer. Assuming negligible changes in the core diameter, the shell thicknesses were calculated from statistical TEM analyses of the full QD sizes. As an additional measure, sizes were calculated from the expected reaction yield.

B. Raman spectroscopy

The QD solutions were drop-casted on silicon wafers. All spectra were recorded in a confocal backscattering geometry. A 514 nm ArKr ion laser (Coherent) served as an excitation source, and a HORIBA LabRAM HR Raman microscope equipped with a 1800 grooves/mm grating and a Peltier-cooled CCD was used to acquire the Raman spectra. The laser power was kept at a few hundred microwatts on a diffraction limited spot to avoid sample heating or destruction. Reference spectra were taken from several sample spots, showing no significant degradation. Each set of spectra was calibrated using neon lines.

III. EXPERIMENTAL RESULTS AND DISCUSSION

Figure 1(a) summarizes the optical properties of the core/shell QDs studied here. An exemplary TEM image is displayed in Fig. 1(b). The QDs are of uniform size and can be well-resolved by TEM, but the limited element contrast does not permit to differentiate between core and shell. This is possible with Raman spectroscopy. The different reduced masses of the ions contributing to the phonon vibrations result in different frequencies of the corresponding Raman bands. Figure 2 displays exemplary Raman spectra of the three systems, plain InP QDs, InP/ZnSe core/shell QDs, and InP/ZnS core/shell QDs. The Raman spectrum of the plain InP QDs consists of two sub-bands centered around 300 cm^{-1} and 340 cm^{-1}. The two bands are commonly assigned to the longitudinal optical phonon (LO) and the transverse optical phonon (TO) of InP.[18] In the case of InP/ZnSe QDs, the lighter InP lattice has its Raman-active LO mode at higher frequencies than ZnSe. In the Raman spectra, the ZnSe shell reflects as a broad Raman band around 210 cm^{-1} and can be assigned to the ZnSe LO.[15]

In the case of InP/ZnS QDs, the situation is different because the ZnS LO and the InP LO have frequencies in a similar regime, leading to a broad Raman band around 350 cm^{-1}.[22] All observed LO frequencies of core/shell QDs differ from the plain core and bulk values because of strain due to lattice reconstruction. A compression of the lattice results in a shift to higher frequencies, while tensile strain lowers the frequency. Monitoring the evolution of the LO frequency with increasing shell dimensions gives direct access to the mismatch-induced strain. Figure 3 summarizes the evolution of the Raman spectra of InP/ZnSe QDs with increasing shell thicknesses. The Raman bands shift to higher frequencies with increasing thickness of the ZnSe shell. In addition, the shell-related Raman band gains in relative intensity and narrows. Starting from thicknesses of 5 monolayers and above, two modes can be resolved
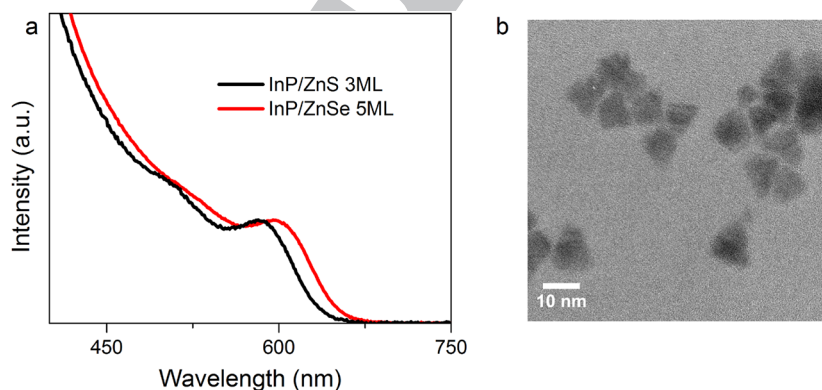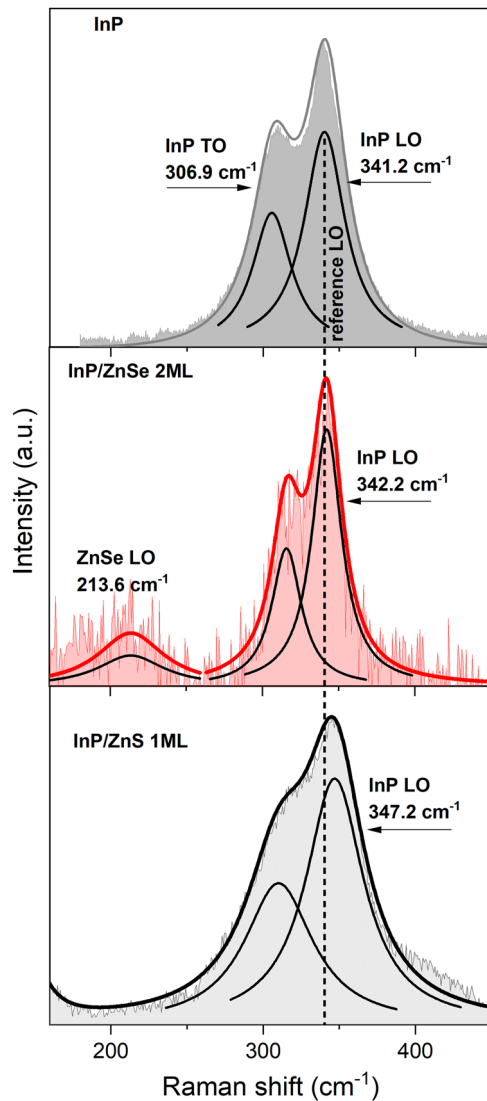

FIG. 1. (a) Absorption spectra of InP QDs with 3 monolayer ZnS and 5 monolayer ZnSe shells. The InP absorption peaks around 600 nm and the wide-bandgap ZnSe or ZnS absorb at shorter wavelengths. (b) TEM image of InP/ZnSe core/shell QDs with a shell thickness of 13 monolayers, resulting in a total diameter of ~11 nm.

FIG. 2. Top: Raman spectrum of plain InP QDs. The bold gray line is a best fit of the intensity to a sum of two Lorentzian functions. The black solid lines are the individual Lorentzian functions used for the fit, offset for clarity. Middle: Raman spectrum of InP QDs with a 2 monolayer ZnSe shell. The red line is a best fit of the intensity to a sum of three Lorentzian functions. The black solid lines are the individual Lorentzian functions used for the fit, offset for clarity. Bottom: Raman spectrum of InP QDs with a monolayer ZnS shell. The bold black line is a best fit of the intensity to a sum of two Lorentzian functions. The black solid lines are the individual Lorentzian functions used for the fit, offset for clarity.

within the shell-related band. The more prominent band can be assigned to the ZnSe LO and the low-frequency shoulder to the ZnSe TO[23] (see the supplementary material for more details). For a more quantitative discussion, the widths and center frequencies of the LO bands can be determined by fitting Lorentzian functions to
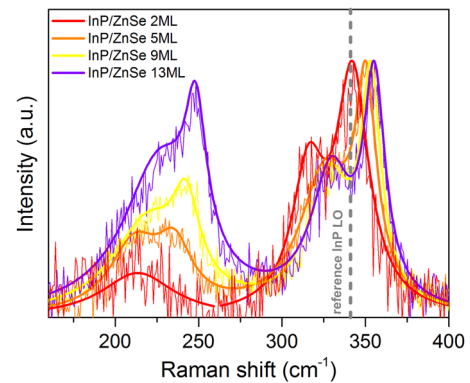
FIG. 3. Raman spectra of InP/ZnSe core/shell QDs with different amounts of shell layers as indicated by the figure legend. The data were normalized to the intensity in the frequency region of the InP LO band. Solid lines are fits to the data, and the InP LO frequency of plain InP QDs is shown as a dashed line.

the spectra. For samples with shell thicknesses above 2 monolayers, each Raman band was fitted with the sum of two Lorentzian functions, and Fig. 4 displays the results for the core- and shell-related LO Raman bands. Included in the figure are the LO frequencies of bulk ZnSe of 250 cm^{-1} and of plain InP QDs.[22,24] In the case of the InP core, the LO shift to higher frequencies is a shift away from the plain QD reference value, while the shell's LO frequency approaches the bulk value for increasing layer numbers. The frequency shifts $\frac{\Delta \omega}{\omega}$ can be related to relative lattice constant changes $\frac{\Delta a}{a}$ by

$$\frac{\Delta \omega}{\omega} = \left(1 + 3\frac{\Delta a}{a}\right)^{-\gamma} - 1. \quad (1)$$

Here, γ is the Grüneisen parameter, which describes the hydrostatic component of strain $\gamma = -\frac{\partial \ln \omega}{\partial \ln V}$, where V is the crystal volume.[25,26] For InP, the mode Grüneisen parameter for the LO is $\gamma_{InP} = 1.24$ and $\gamma_{ZnSe} = 0.85$ for ZnSe.[27,28] The outcome of the evaluation of Eq. (1) is summarized in Fig. 5 and shows a behavior very similar to the more established material combination CdSe/CdS.[17,29–31] The smaller lattice constant of ZnSe (5.62 Å[32]) relative to InP (5.87 Å[33]) leads to compressive strain in the core and tensile strain in the shell material. For the core, the strain builds up with increasing shell thickness and then begins to saturate. This is especially important when aiming at investigating fundamental material differences.[15] For the shell, the initial layer is heavily strained and more shell material allows the strain to relax, leading to a reduction of the relative amount of strain within the lattice. The increase of shell lattice homogeneity is also reflected in the reduction of the ZnSe LO Raman bandwidth [Fig. 3(a)].

Raman spectra of InP/ZnS QDs with gradually increasing shell thickness are displayed in Fig. 6. The lighter sulfur in comparison to selenium leads to higher ZnS LO frequencies; the bulk value is reported at 350 cm^{-1} in the range of the InP LO.[22] This results in mixed Raman bands even for thick shells. Owing to this uncertainty, the shell-related LO cannot be discussed. To estimate the InP LO
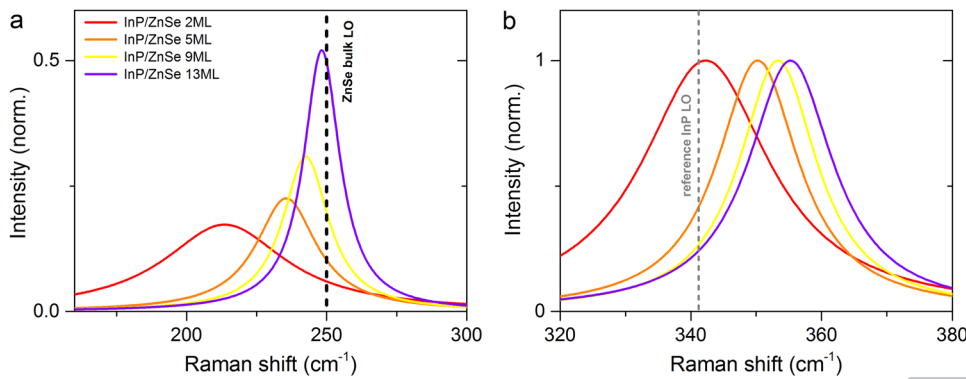
FIG. 4. Lorentzian functions used to fit the LO bands in the data presented in Fig. 3 in the frequency of (a) the ZnSe shell and (b) the InP core. The LO frequencies of bulk ZnSe and plain InP QDs are indicated as dashed lines.

frequencies, the fundamental Raman band can be fitted with the sum of three Lorentzian functions. Restricting the free parameters to reasonable values led to robust values for the InP LO frequency. Details are presented in the supplementary material. The Lorentzian functions used to fit the InP LO band are displayed in Fig. 7(a). The evolution of the corresponding strain in the InP core is displayed in Fig. 7(b). ZnS also has a smaller lattice constant than InP ($a_{ZnS} = 5.4$ Å).[33] As for ZnSe, the addition of ZnS layers compressively strains the InP core and the amount of strain increases with increasing shell dimensions. The strong impact on the core could be attributed to the larger lattice mismatch. However, significant general differences are observed for the shell: even 5 and 9 monolayers of ZnSe are strained above 1% (Fig. 5), while even the smallest volumes of ZnS are strained below 0.5%, following an evaluation of Eq. (1) with $\gamma_{ZnS} = 0.95$[27] and the potential LO frequency range. However, note that the assignment of the ZnS-related strain values is less accurate than for the ZnSe shells, as the fit of the fundamental Raman band with three Lorentzian functions is less robust. Still, the order of magnitude is valid. Regarding the core, the strain buildup with increasing shell volumes differs between the materials. Even monolayer ZnS shells induce measurable strain, and the buildup is more drastic than with ZnSe shells.

The observed difference can be qualitatively explained by the mechanical properties of the materials. In the linear regime, the relation between stress at the interface and the deformation of the lattice is given by the material's Young's modulus.[34,35] The stiffness of ZnS is higher than that of ZnSe ($9.7 \cdot 10^{10}$ Nm^{-2} and $7.4 \cdot 10^{10}$ Nm^{-2}, respectively).[32,36] Assuming comparable stress from the reconstruction of the InP lattice, this results in a higher relative stress on the InP core. Because of the higher Young's modulus, small amounts of ZnS deform less than those of ZnSe at the interface with InP. The softer ZnSe requires more material to develop from a quasiamorphous layer to a more uniform lattice. Comparable effects can be expected for other material combinations, too. However, as numerical studies are missing, a quantitative comparison with the more established CdSe-based QDs is problematic. CdSe has a much lower Young's modulus than InP ($5.1 \cdot 10^{10}$ Nm^{-2} vs $7.1 \cdot 10^{10}$ Nm^{-2}), and the exact impact is hard to estimate.[37] A comparison of CdSe/CdS core/shell QDs with CdSe/ZnSe QDs and the InP-based counterparts with focus on both components would be very interesting. There, similar trends for the buildup and relaxation of strain in core and shell could be observed. Also, computational studies are highly encouraged.
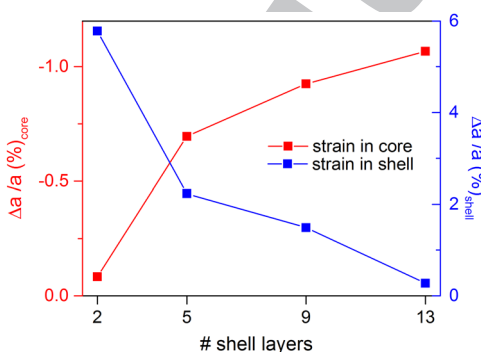

FIG. 5. Strain in the core and shell of InP/ZnSe QDs vs amount of shell layers from evaluating Eq. (1), with the frequency shifts obtained from the fits presented in Fig. 3. Note the different sign for core and shell.
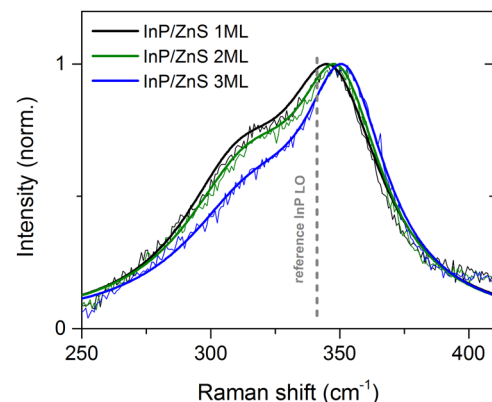

FIG. 6. Raman spectra of InP/ZnS core/shell QDs with increasing shell thickness as indicated by the figure legend. The solid lines are fits to the data, and the InP LO frequency of plain InP QDs is shown as a dashed line.
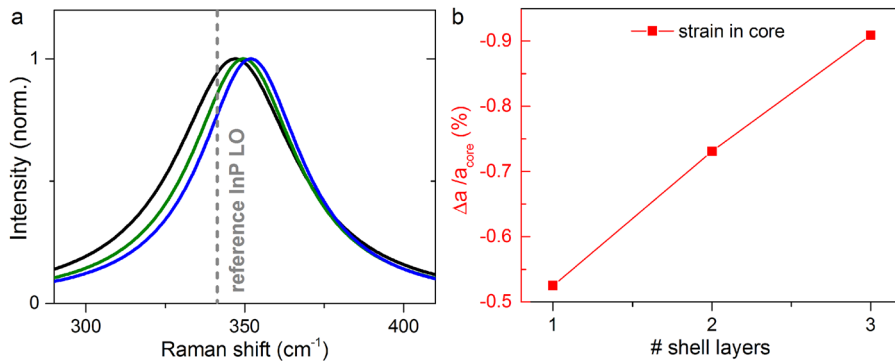
FIG. 7. (a) Lorentzian functions used to fit the InP LO component of the data presented in Fig. 6. The InP LO frequency of plain InP QDs is indicated as a dashed line. (b) Resulting strain values for the InP core vs ZnS shell layer number.

IV. CONCLUSION

We have investigated the evolution of lattice-mismatch induced strain with the addition of ZnS and ZnSe shells on InP QDs. The lattice mismatch leads to compressive strain in the InP core and tensile strain in the shell material. Larger shell volumes allow the shell to grow more homogeneously and relax strain across the lattice, increasing the effect on the core. Despite comparable lattice constants, ZnS and ZnSe behave systematically different. The larger Young's modulus of ZnS makes the material requiring less volume to build up stress on the core, where ZnSe requires at least two monolayers to develop a crystalline lattice and a significant effect on the core. This effect will also be of relevance for other material combinations and makes the material stiffness another parameter to consider when optimizing core/shell QDs for strain.

SUPPLEMENTARY MATERIAL

See the supplementary material for details on the nanocrystal size determination, the fitting procedure, and additional Raman spectra.

ACKNOWLEDGMENTS

REFERENCES

[1] Y. Yang, Y. Zheng, W. Cao, A. Titov, J. Hyvonen, J. R. Manders, J. Xue, P. H. Holloway, and L. Qian, "High-efficiency light-emitting devices based on quantum dots with tailored nanostructures," Nat. Photonics **9**(4), 259–266 (2015).

[2] J. M. Pietryga, Y.-S. Park, J. Lim, A. F. Fidler, W. K. Bae, S. Brovelli, and V. I. Klimov, "Spectroscopic and device aspects of nanocrystal quantum dots," Chem. Rev. **116**(18), 10513–10622 (2016).

[3] T. Shen, L. Bian, B. Li, K. Zheng, T. Pullerits, and J. Tian, "A structure of CdS/Cu$_x$S quantum dots sensitized solar cells," Appl. Phys. Lett. **108**(21), 213901 (2016).

[4] Z. Yang, M. Gao, W. Wu, X. Yang, X. W. Sun, J. Zhang, H.-C. Wang, R.-S. Liu, C.-Y. Han, H. Yang, and W. Li, "Recent advances in quantum dot-based light-emitting devices: Challenges and possible solutions," Mater. Today **24**, 69–93 (2019).

[5] D. V. Talapin, J.-S. Lee, M. V. Kovalenko, and E. V. Shevchenko, "Prospects of colloidal nanocrystals for electronic and optoelectronic applications," Chem. Rev. **110**(1), 389–458 (2010).

[6] R. Xie, D. Battaglia, and X. Peng, "Colloidal InP nanocrystals as efficient emitters covering blue to near-infrared," J. Am. Chem. Soc. **129**(50), 15432–15433 (2007).

[7] P. Reiss, M. Protière, and L. Li, "Core/shell semiconductor nanocrystals," Small **5**(2), 154–168 (2009).

[8] V. Brunetti, H. Chibli, R. Fiammengo, A. Galeone, M. A. Malvindi, G. Vecchio, R. Cingolani, J. L. Nadeau, and P. P. Pompa, "InP/ZnS as a safer alternative to CdSe/ZnS core/shell quantum dots: *In vitro* and *in vivo* toxicity assessment," Nanoscale **5**(1), 307–317 (2012).

[9] S. J. Soenen, B. B. Manshian, T. Aubert, U. Himmelreich, J. Demeester, S. C. De Smedt, Z. Hens, and K. Braeckmans, "Cytotoxicity of cadmium-free quantum dots and their use in cell bioimaging," Chem. Res. Toxicol. **27**(6), 1050–1059 (2014).

[10] K. Gong and D. F. Kelley, "A predictive model of shell morphology in CdSe/CdS core/shell quantum dots," J. Chem. Phys. **141**(19), 194704 (2014).

[11] A. M. Smith, A. M. Mohs, and S. Nie, "Tuning the optical and electronic properties of colloidal nanocrystals by lattice strain," Nat. Nanotechnol. **4**(1), 56–63 (2009).

[12] C. Phadnis, K. G. Sonawane, A. Hazarika, and S. Mahamuni, "Strain-induced hierarchy of energy levels in CdS/ZnS nanocrystals," J. Phys. Chem. **119**(42), 24165–24173 (2015).

[13] V. Kocevski, O. Eriksson, C. Gerard, D. D. Sarma, and J. Rusz, "Influence of dimensionality and interface type on optical and electronic properties of CdS/ZnS core-shell nanocrystals—A first-principles study," J. Chem. Phys. **143**(16), 164701 (2015).

[14] F. Pietra, L. De Trizio, A. W. Hoekstra, N. Renaud, M. Prato, F. C. Grozema, P. J. Baesjou, R. Koole, L. Manna, and A. J. Houtepen, "Tuning the lattice parameter of In$_X$Zn$_Y$P for highly luminescent lattice-matched core/shell quantum dots," ACS Nano **10**(4), 4754–4762 (2016).

[15] M. Rafipoor, D. Dupont, H. Tornatzky, M. D. Tessier, J. Maultzsch, Z. Hens, and H. Lange, "Strain engineering in InP/(Zn,Cd)Se core/shell quantum dots," Chem. Mater. **30**(13), 4393–4400 (2018).

[16] A. V. Baranov, Y. P. Rakovich, J. F. Donegan, T. S. Perova, R. A. Moore, D. V. Talapin, A. L. Rogach, Y. Masumoto, and I. Nabiev, "Effect of ZnS shell thickness on the phonon spectra in CdSe quantum dots," Phys. Rev. B **68**(16), 165306 (2003).

[17] N. Tschirner, H. Lange, A. Schliwa, A. Biermann, C. Thomsen, K. Lambert, R. Gomes, and Z. Hens, "Interfacial alloying in CdSe/CdS heteronanocrystals: A Raman spectroscopy analysis," Chem. Mater. **24**(2), 311–318 (2012).

[18] M. J. Seong, O. I. Mićić, A. J. Nozik, A. Mascarenhas, and H. M. Cheong, "Size-dependent Raman study of InP quantum dots," Appl. Phys. Lett. **82**(2), 185–187 (2003).

[19] V. M. Dzhagan, M. Ya Valakh, A. E. Raevskaya, A. L. Stroyuk, S. Ya Kuchmiy, and D. R. T. Zahn, "Resonant Raman scattering study of CdSe nanocrystals passivated with CdS and ZnS," Nanotechnology **18**(28), 285701 (2007).

[20] A. Biermann, T. Aubert, P. Baumeister, E. Drijvers, Z. Hens, and J. Maultzsch, "Interface formation during silica encapsulation of colloidal CdSe/CdS quantum dots observed by *in situ* Raman spectroscopy," J. Chem. Phys. **146**(13), 134708 (2017).

[21] M. D. Tessier, D. Dupont, K. De Nolf, J. De Roo, and Z. Hens, "Economic and size-tunable synthesis of InP/ZnE (E = S, Se) colloidal quantum dots," Chem. Mater. **27**(13), 4893–4898 (2015).

[22] M. Dimitrievska, H. Xie, A. J. Jackson, X. Fontané, M. Espíndola-Rodríguez, E. Saucedo, A. Pérez-Rodríguez, A. Walsh, and V. Izquierdo-Roca, "Resonant Raman scattering of $ZnS_X Se_{1-X}$ solid solutions: The role of S and Se electronic states," Phys. Chem. Chem. Phys. **18**(11), 7632–7640 (2016).

[23] M. Shakir, S. K. Kushwaha, K. K. Maurya, G. Bhagavannarayana, and M. A. Wahab, "Characterization of ZnSe nanoparticles synthesized by microwave heating process," Solid State Commun. **149**(45), 2047–2049 (2009).

[24] R. K. Ram, S. S. Kushwaha, and A. Shukla, "Phonon assignments in II-VI and III-V semiconductor compounds having zincblende-type structure," Phys. Status Solidi (b) **154**(2), 553–564 (1989).

[25] *Light Scattering in Solids IV*, edited by M. Cardona and G. Güntherodt (Springer Berlin Heidelberg, 1984).

[26] G. Scamarcio, M. Lugará, and D. Manno, "Size-dependent lattice contraction in $CdS_{1-x}Se_x$ nanocrystals embedded in glass observed by Raman scattering," Phys. Rev. B **45**(23), 13792–13795 (1992).

[27] R. Trommer, H. Müller, M. Cardona, and P. Vogl, "Dependence of the phonon spectrum of InP on hydrostatic pressure," Phys. Rev. B **21**(10), 4869–4878 (1980).

[28] R. M. Feenstra and S. W. Hla. *2.3.12 InP, Indium Phosphide* (Springer Berlin Heidelberg, 2015).

[29] V. M. Dzhagan, M. Y. Valakh, A. G. Milekhin, N. A. Yeryukov, D. R. T. Zahn, E. Cassette, T. Pons, and B. Dubertret, "Raman- and IR-active phonons in CdSe/CdS core/shell nanocrystals in the presence of interface alloying and strain," J. Phys. Chem. **117**(35), 18225–18233 (2013).

[30] L. Lu, X.-L. Xu, W.-T. Liang, and H.-F. Lu, "Raman analysis of CdSe/CdS core-shell quantum dots with different CdS shell thickness," J. Phys.: Condens. Matter **19**(40), 406221 (2007).

[31] V. M. Dzhagan, Y. M. Azhniuk, A. G. Milekhin, and D. R. T. Zahn, "Vibrational spectroscopy of compound semiconductor nanocrystals," J. Phys. D: Appl. Phys. **51**(50), 503001 (2018).

[32] *Zinc Sulfide (ZnS) Third-Order Elastic Constants, Young's Modulus, Poisson's Ratio, Grueneisen Parameters*, edited by O. Madelung, U. Rössler, and M. Schulz (Springer Berlin Heidelberg, Berlin, Heidelberg, 1999).

[33] *Indium Phosphide (InP) Lattice Parameters, Thermal Expansion*, edited by O. Madelung, U. Rössler, and M. Schulz (Springer Berlin Heidelberg, Berlin, Heidelberg, 2001).

[34] B. Budiansky, "On the elastic moduli of some heterogeneous materials," J. Mech. Phys. Solids **13**(4), 223–227 (1965).

[35] Z.-Q. Wang, Y.-P. Zhao, and Z.-P. Huang, "The effects of surface tension on the elastic properties of nano structures," Int. J. Eng. Sci. **48**(2), 140–150 (2010).

[36] U. Rössler, *ZnS: Lattice Parameters* (Springer Berlin Heidelberg, Berlin, Heidelberg, 2013).

[37] D. Strauch, *CdSe: Bulk Modulus, Compressibility: Datasheet from Landolt-Börnstein - Group III Condensed Matter* (Springer Berlin Heidelberg, Berlin, Heidelberg, 2012).